

# A VUV Photoionization Study of the Formation of the Indene Molecule and Its Isomers

Fangtong Zhang and Ralf I. Kaiser\*

Department of Chemistry, University of Hawaii at Manoa, Honolulu, Hawaii 96822

Vadim V. Kislov and Alexander M. Mebel\*

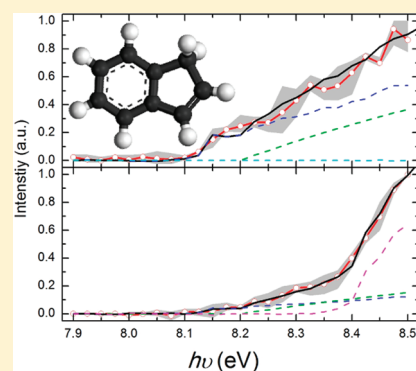
Department of Chemistry and Biochemistry, Florida International University MMC, Miami, Florida 33199

Amir Golan and Musahid Ahmed\*

Chemical Sciences Division, Lawrence Berkeley National Laboratory, Berkeley, California 94720

**ABSTRACT:** The aromatic indene molecule ( $C_9H_8$ ) together with its acyclic isomers (phenylallene, 1-phenyl-1-propyne, and 3-phenyl-1-propyne) were formed via a “directed synthesis” in situ utilizing a high-temperature chemical reactor under combustion-like conditions (300 Torr, 1200–1500 K) through the reactions of the phenyl radical ( $C_6H_5$ ) with propyne ( $CH_3CCH$ ) and allene ( $H_2CCCH_2$ ). The isomer distributions were probed utilizing tunable vacuum ultraviolet (VUV) radiation from the Advanced Light Source by recording the photoionization efficiency (PIE) curves at mass-to-charge of  $m/z = 116$  ( $C_9H_8^+$ ) of the products in a supersonic expansion for both the phenyl-allene and phenyl-propyne systems; branching ratios were derived by fitting the recorded PIE curves with a linear combination of the PIE curves of the individual  $C_9H_8$  isomers. Our data suggest that under our experimental conditions, the formation of the aromatic indene molecule via the reaction of the phenyl radical with allene is facile and enhanced compared to the phenyl-propyne system by a factor of about 7. Reaction mechanisms and branching ratios are explained in terms of new electronic structure calculations. Our newly developed high-temperature chemical reactor presents a versatile approach to study the formation of combustion-relevant polycyclic aromatic hydrocarbons (PAHs) under well-defined and controlled conditions.

**SECTION:** Dynamics, Clusters, Excited States



The energetics and dynamics of the reactions of aromatic radicals (ARs) such as the phenyl radical ( $C_6H_5$ ) with unsaturated hydrocarbons are of paramount importance in untangling the formation of polycyclic aromatic hydrocarbons (PAHs) from the “bottom up” in combustion flames<sup>1,2</sup> and in carbon-rich circumstellar envelopes.<sup>3</sup> Due to their inherent thermodynamical stability, ARs can reach high concentrations in flames; this makes them important reactants to be involved in the formation of PAHs and carbonaceous nanostructures. Reaction mechanisms are suggested to involve ARs such as phenyl<sup>4</sup> with unsaturated C3 and C4 hydrocarbons possibly forming bicyclic aromatic hydrocarbon molecules with indene ( $C_9H_8$ ) and naphthalene ( $C_{10}H_8$ ) cores. However, no experiment has been conducted so far in which a PAH (-like) species is formed as a result of a *directed* and *controlled* synthesis in the gas phase under combustion-like conditions. Computational predictions do exist. For instance, Fascella et al.<sup>5</sup> investigated the reaction of the phenyl radical with 1,3-butadiene ( $C_4H_6$ ), theoretically suggesting that over the complete temperature range of 500–2500 K, 1,4-dihydronaphthalene ( $C_{10}H_{10}$ ) was the predominant product.

Considering the indene molecule ( $C_9H_8$ ), Vereecken et al.<sup>6–8</sup> theoretically estimated the product distributions of the reactions of phenyl with propyne ( $CH_3CCH$ ) and allene ( $H_2CCCH_2$ ). The authors proposed that indene should be the dominant product at low pressures and temperatures up to 500 K (Figure 1). At higher temperatures of up to 2000 K, the branching ratios strongly depend on the pressure (1–100 atm) and effective temperature leading to  $C_9H_8$  isomers indene, 1-phenyl-1-propyne, 3-phenyl-1-propyne, and phenylallene; additional exit channels of phenylacetylene ( $C_6H_5CCH$ ) plus the methyl radical ( $CH_3$ ) and benzene ( $C_6H_6$ ) plus the propargyl radical ( $H_2CCCH$ ) were also proposed. At temperatures of 3000–4000 K, indene was found to be only a small fraction of all products formed. The latter finding is consistent with recent crossed molecular beam experiments conducted at collision energies of about 150 kJ mol<sup>-1</sup>, suggesting that 1-phenyl-1-propyne and phenylallene are

**Received:** May 26, 2011

**Accepted:** June 28, 2011

**Published:** June 28, 2011

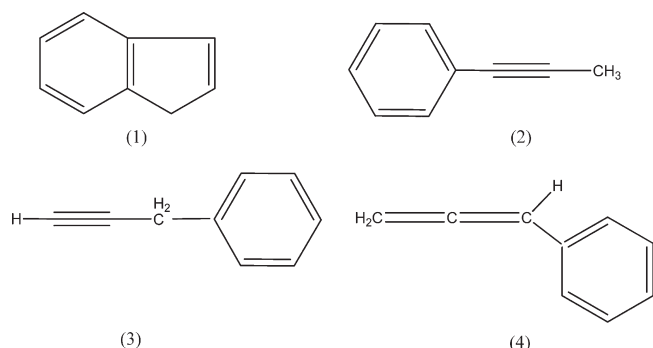


**Figure 1.** Structures of distinct  $C_9H_8$  isomers: indene (1), 1-phenyl-1-propyne (2), 3-phenyl-1-propyne (3), and phenylallene (4).

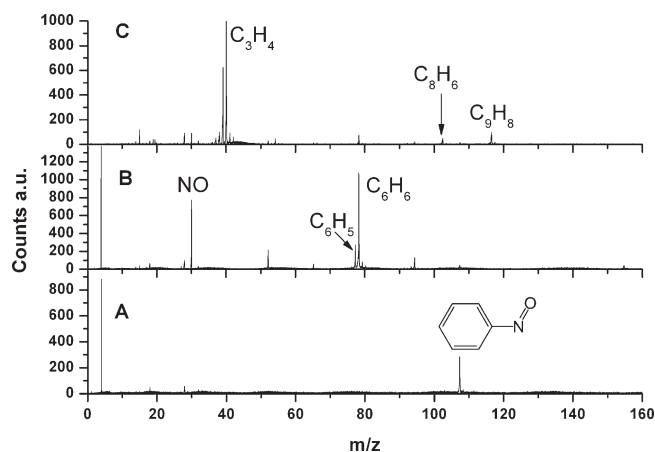


**Figure 2.** Mass spectra of prominent species in the helium-seeded supersonic nitrosobenzene beam without heating the nozzle [nitrosobenzene ( $C_6H_5NO$ )] (A), with heating the nozzle [nitrogen monoxide (NO); phenyl radical ( $C_6H_5$ ); benzene ( $C_6H_6$ )] (B), and in the heated nitroso benzene beam entrained in propyne [propyne ( $C_3H_4$ ); phenylacetylene ( $C_8H_6$ );  $C_9H_8$  isomers] (C) recorded at a photon energy of 10 eV.

the dominating  $C_9H_8$  isomers formed in the reactions of phenyl radicals with propyne and allene, respectively, under single collision conditions.<sup>9</sup>

In this Letter, we present the first experimental evidence that the aromatic indene molecule together with its acyclic isomers can be formed via a “directed synthesis” through the reaction of the phenyl radical with propyne and allene under combustion-relevant conditions (300 Torr, 1200–1500 K). Utilizing a high-temperature “chemical reactor”, we synthesize the isomers in situ via reaction of pyrolytically<sup>10</sup> generated phenyl radicals ( $C_6H_5$ ) with two  $C_3H_4$  isomers—allene ( $H_2CCCH_2$ ) and propyne ( $CH_3CCH$ )—followed by isomerization and/or fragmentation of the initial  $C_9H_9$  complexes. Note that for distinct structural isomers, the adiabatic ionization energy (IE) and the corresponding photoionization efficiency (PIE) curves, which report the ion signal of  $m/z = 116$  ( $C_9H_8^+$ ) of a distinct isomer versus the photon energy, can differ dramatically.<sup>11,12</sup> By photoionizing the neutral  $C_9H_8$  products in the supersonic molecular beam via tunable vacuum ultraviolet (VUV) radiation from the Advanced Light Source at various photon energies, we measured PIEs of  $m/z = 116$  ( $C_9H_8^+$ ) in the propyne ( $PIE_{MA}$ ) and allene ( $PIE_{AL}$ ) experiments. These PIE curves are the result of a linear

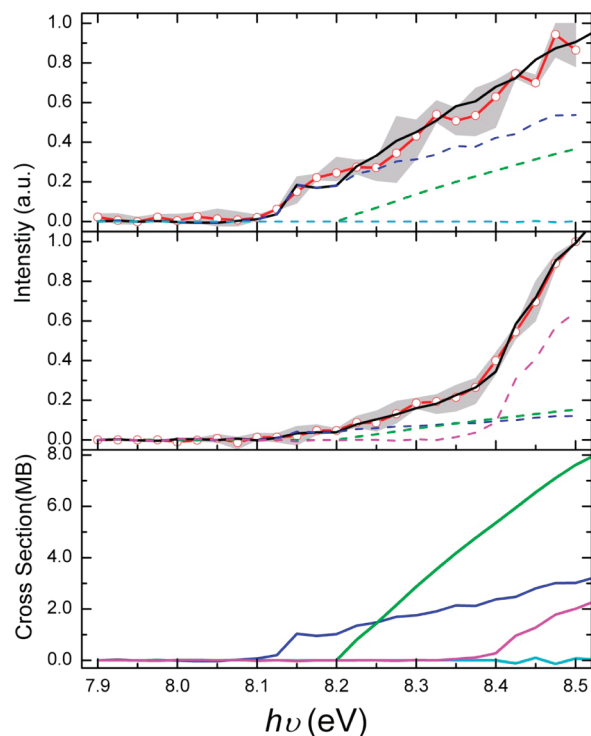


**Figure 3.** Upper panel: Red circles and line are the PIE data obtained in the phenyl–allene system at  $m/z = 116$ . The black line presents the cumulative simulated PIE from the individual PIE curves of indene (1) (blue), phenylallene (4) (green), and 3-phenyl-1-propyne (3) (cyan) with branching ratios listed in Table 1. Center panel: Red circles and line are the PIE data obtained in the phenyl–propyne system at  $m/z = 116$ . The black line presents the cumulative simulated PIE from the individual PIE curves of indene (1) (blue), phenylallene (4) (green), and 1-phenyl-1-propyne (magenta) with branching ratios listed in Table 1. Lower panel: individual PIE curves of four  $C_9H_8$  isomers: indene (1) (blue), phenylallene (4) (green), 1-phenyl-1-propyne (2) (magenta), and 3-phenyl-1-propyne (3) (cyan). The shaded area represents the  $1\sigma$  error limits as derived from averaging four scans from 7.9 to 8.5 eV.

**Table 1. Branching Ratios of Distinct  $C_9H_8$  Isomers Formed in the Phenyl–Allene and Phenyl–Propyne Systems Utilizing a Chemical Reactor at 300 Torr and 1200–1500 K.**

reactant	indene	phenylallene	1-phenyl-1-propyne	3-phenyl-1-propyne
allene	$71 \pm 10\%$	$19 \pm 5\%$	0	$<10 \pm 5\%$
propyne	$10 \pm 5\%$	$8 \pm 5\%$	$82 \pm 10\%$	0

combination of PIE curves of the individual  $C_9H_8$  isomers present in the supersonic beams, and hence we can identify the  $C_9H_8$  products formed in the reactions of phenyl radicals with propyne and allene, and establish their branching ratios.

The mass spectra of the species formed in the supersonic expansion and the PIE curves of  $m/z = 116$  ( $C_9H_8^+$ ) recorded in the propyne ( $PIE_{MA}$ ) and allene ( $PIE_{AL}$ ) experiments are compiled in Figures 2 and in Figure 3, respectively. Figure 3 depicts data over a range of photon energies from 7.9 to 8.5 eV together with the PIE curves of the individual  $C_9H_8$  isomers 1–4 (Figure 1).<sup>13</sup> The PIE curves for the allene (upper) and propyne (center) system differ strongly with  $PIE_{AL}$  showing an intense onset of the ion signal at about 8.1 eV compared to a shallow increase at 8.1 eV for  $PIE_{MA}$ . Among all  $C_9H_8$  isomers, the

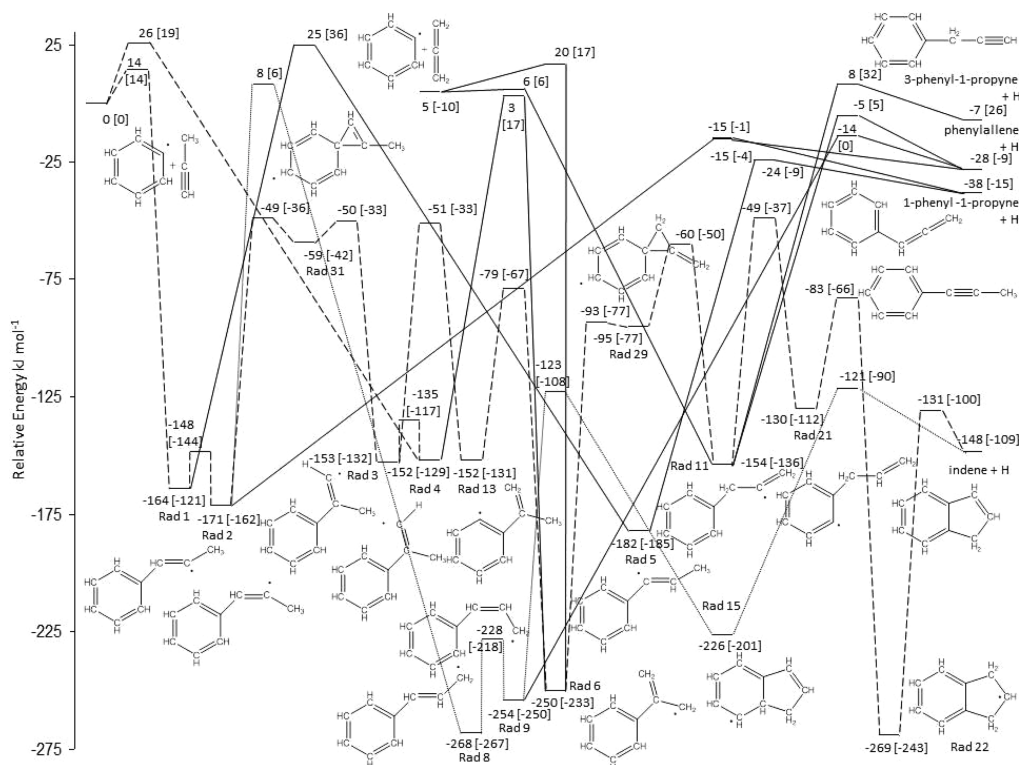


**Figure 4.** Relevant sections of the  $C_9H_9$  PES accessed in the reactions of the phenyl radical with allene and propyne leading to four  $C_9H_8$  isomers. All relative energies (in  $\text{kJ mol}^{-1}$ ) were calculated at the G3(MP2,CC)//B3LYP/6-311+G\*\* + ZPE(B3LYP/6-311+G\*\*) level of theory. The labels of the reaction intermediates Rad and the energetics in square brackets were taken from refs 6–8.

indene molecule (1) depicts the lowest IE of  $8.15 \pm 0.05$  eV,<sup>14</sup> which correlates nicely with the onset of the rise of both PIE curves. A detailed analysis of the PIE curves suggests that in case of the phenyl–allene system, indene represents the dominating  $C_9H_8$  isomer formed with  $71 \pm 10\%$  followed by phenylallene and 3-phenyl-1-propyne (Table 1). These branching ratios are distinctively different from those derived for the phenyl–propyne system. Here, indene and phenylallene are relatively minor products with the 1-phenyl-1-propyne isomer being the dominant product formed. In an attempt to rationalize the formation of the indene molecule together with the distinct branching ratios of the isomers formed in both systems, we took a closer look at the underlying potential energy surfaces (PESs). Figure 4 compiles the relevant sections of the PESs for the reactions of the phenyl radical with propyne and allene leading to four  $C_9H_8$  isomers. All optimized structures were taken from density functional calculations in previous works,<sup>6–8</sup> but their relative energies were refined here using a chemically accurate G3-type computational scheme.

Considering the phenyl–propyne system, electronic structure calculations<sup>6–8</sup> suggest that the phenyl radical adds with its radical center to the sterically less-hindered C1-position of the propyne molecule forming a reaction intermediate Rad 1, which undergoes a rapid cis–trans isomerization to Rad 2. The latter can emit a hydrogen atom either from the acetylenic carbon atom or from the methyl group of the propyne moiety leading to the formation of 1-phenyl-1-propyne and phenylallene, respectively, via tight transition states. The energetically least favorable isomer, the 3-phenyl-1-propyne molecule, cannot be accessed via the decomposition of Rad 2. The indene molecule can only be synthesized via a complex series of isomerization steps from

Rad 2 involving eight intermediates along the dashed line. The isomerization sequence Rad 8  $\rightarrow$  Rad 9  $\rightarrow$  Rad 15 as depicted in the dotted line presents an alternative pathway to form indene plus atomic hydrogen. A comparison of these theoretically feasible pathways with the experimental data suggests the following scenario: In the chemical reactor, the phenyl radical adds to the C1-carbon atom of propyne forming Rad 1, which isomerizes to Rad 2. The lifetime of the majority of the Rad 2 intermediates is likely quite short so that a predominant fraction of Rad 2 decomposes to 1-phenyl-1-propyne, i.e., via hydrogen emission from the C1 carbon atom; here, the energy randomization in Rad 2 is incomplete, thus significantly inhibiting an “energy flow” across the carbon–carbon skeleton to the carbon–hydrogen bonds of the methyl group; this in turn would reduce the formation of phenylallene compared to 1-phenyl-1-propyne as observed experimentally. However, keeping in mind that the experiments are not conducted under single collision conditions (multiple collisions can deactivate the reaction intermediates thus increasing their lifetime), the experimental data suggests that a smaller fraction of the Rad 2 intermediates form the indene molecule involving multiple isomerization steps; considering the heights of the barriers to access Rad 31 (dashed route) and Rad 8 (dotted route), the formation of the indene molecule should proceed preferentially via the dashed line. This conclusion is in line with previous computations.<sup>6–8</sup>

In the case of the phenyl–allene system, the calculations predict an addition of the phenyl radical with its radical center to the C1 or C2 (central) carbon atom of the allene molecule leading to intermediates Rad 11 and Rad 6, respectively. Rad 11 could eliminate a hydrogen atom from the C1 or C3 carbon atom of the allene moiety forming either phenylallene or 3-phenyl-1-propyne.

Note that similar to the phenyl-propyne system, if the energy randomization of the majority of Rad 11 is incomplete, thus largely inhibiting an effective energy transfer to the terminal CH<sub>2</sub> group, phenylallene should be formed preferentially compared to 3-phenyl-1-propyne. This was clearly observed experimentally. The major difference in the reactions of phenyl with propyne and allene presents a significantly increased fraction of indene formation in the allene reaction. A closer look at the relevant part of the PES might explain this finding. Upon formation of Rad 11, only two isomerization steps to Rad 22 are necessary prior to the decomposition to the indene molecule; four steps are necessary if Rad 6 is formed initially. On the other hand, the formation of indene in the phenyl-propyne system involves eight reaction steps, among them the common intermediate Rad 11. Therefore, the experimental results and the computations suggest that Rad 11 likely presents a common intermediate in the formation of the indene molecule in the reactions of the phenyl radical with both propyne and allene. Considering that only two additional reaction steps are involved in the indene synthesis in the phenyl-allene system, but eight in the phenyl-propyne reaction, indene is preferentially formed in the reaction of phenyl radicals with allene as verified experimentally (Table 1).

To summarize, our experiments utilizing a high-temperature chemical reactor established for the first time that the aromatic indene molecule can be synthesized under combustion-like conditions via a directed synthesis through the reactions of the phenyl radical with allene and propyne, with the allene system giving 7 times higher yields. Therefore, these pathways may also account for the synthesis of indene in “real” hydrocarbon flames.<sup>15–20</sup> Besides the PAH indene, we also detected three acyclic isomers—phenylallene and 3-phenyl-1-propyne (allene system) and phenylallene and 1-phenyl-1-propyne (propyne system)—and proposed their formation routes. We believe that this thermal chemical reactor will be a convenient source for “directed” synthesis of more complex PAHs via reactions with C3 and C4 hydrocarbons under controlled conditions in future experiments.

## EXPERIMENTAL AND THEORETICAL METHODS

The centerpiece of the experiments is a resistively heated high-temperature “chemical reactor” incorporated into the molecular beams end station<sup>21</sup> at the Chemical Dynamics Beamline (9.0.2.) of the Advanced Light Source. This reactor allows an experimental simulation of combustion-relevant conditions (temperatures, pressures) and chemical reactions to form PAHs and their acyclic isomers in situ. Briefly, a continuous beam of phenyl radicals (C<sub>6</sub>H<sub>5</sub>) was generated in situ via quantitative pyrolysis<sup>10</sup> of nitrosobenzene (C<sub>6</sub>H<sub>5</sub>NO; Aldrich; held at 293 K) seeded in the hydrocarbon carrier gas (allene [H<sub>2</sub>CCCH<sub>2</sub>; 97%; Sigma] or propyne [CH<sub>3</sub>CCH; 98%; Sigma]) expanded at a backing pressure of 300 Torr through a 0.1 mm orifice into a resistively heated silicon carbide (SiC) tube. In the present experiments, a heating current of 1.3 A was applied to the silicon carbide tube resulting in an operating power of 20 W. An external temperature calibration of the pyrolytic source with pure helium carrier gas coupled to a time-of-flight mass spectrometer and chopper wheel suggested temperatures of 1200–1500 K of the silicon carbide tube. Note that the hydrocarbon did not only act as a seeding gas, but also as a reactant with the pyrolytically generated phenyl radicals. We estimated the residence time of the reactants

accounting for the length of the tube (2.0 ± 0.1 cm) and a thermal, non supersonic velocity of the methylacetylene/allene reactants at 1350 ± 150 K inside the tube of 920 ± 50 m s<sup>-1</sup> to be 24 ± 2 μs. Our machine provides an unprecedented tool to analyze these in situ generated PAHs and their isomers. Here, after passing a 2 mm skimmer located 10 mm downstream from the silicon carbide nozzle, quasi continuous tunable VUV radiation from the Advanced Light Source crossed the neutral molecular beam at the extraction region of a Wiley–McLaren reflectron time-of-flight (Re-TOF) mass spectrometer 55 mm downstream. Fragment-free VUV photoionization mass spectrometry—a soft ionization method—is unmatched by traditional ionization techniques utilizing electron impact schemes.<sup>22</sup> The ions of the photoionized molecules were then extracted and collected by a microchannel plate detector in the Re-TOF mode utilizing a multi channel scaler. The PIE curves were obtained by plotting the integrated relevant ion counts at a desired mass-to-charge, *m/z*, versus the photoionization energy between 7.900 and 8.600 eV in steps of 0.025 eV. The signal was normalized to the photon flux. On the basis of known PIE curves of expected PAHs of a well-defined molecular mass and their acyclic isomers (*m/z* = 116; C<sub>9</sub>H<sub>8</sub>), the recorded PIE curves were then fit via a linear combination with known PIE curves of various C<sub>9</sub>H<sub>8</sub> isomers to extract the nature of the products formed and their branching ratios.

In our theoretical calculations of the PESs, we utilized geometries of various species from the previous works<sup>9–11</sup> optimized at the B3LYP/6-311+G\*\* level of theory. To obtain more accurate energies, we applied the G3(MP2,CC)//B3LYP modification<sup>23,24</sup> of the original Gaussian 3 (G3) scheme<sup>25</sup> for high-level single-point energy calculations. The final energies at 0 K were obtained using the B3LYP optimized geometries and zero-point energy (ZPE) corrections according to the following formula 1:

$$E_0[\text{G3(MP2, CC)}] = E[\text{CCSD(T)/6-311G(d,p)}] + \Delta E_{\text{MP2}} + E(\text{ZPE}) \quad (1)$$

where  $\Delta E_{\text{MP2}} = E[\text{MP2/G3large}] - E[\text{MP2/6-311G(d,p)}]$  is the basis set correction, and  $E(\text{ZPE})$  is the zero-point energy.  $\Delta E(\text{SO})$ , a spin-orbit correction, and  $\Delta E(\text{HLC})$ , a higher level correction, from the original G3 scheme were not included in our calculations, as they are not expected to make significant contributions into relative energies. We used the Gaussian 98<sup>26</sup> program package to carry out MP2 calculations, and the MOLPRO 2002<sup>27</sup> program package to perform calculations of spin-restricted coupled cluster RCCSD(T) energies.

## ACKNOWLEDGMENT

This research was supported by the U.S. Department of Energy Office of Science via projects DE-FG02-03-ER15411 (RIK, FZ) and DE-FG02-04ER15570 (VVK, AMM). A.G., M.A., and the A.L.S. are supported by the Director, Office of Energy Research, Office of Basic Energy Sciences, Chemical Sciences Division of the U.S. Department of Energy under Contract No. DE-AC02-05CH11231. We would also like to thank Dr. David Osborn (Sandia) for providing the photoionization curves of the C<sub>9</sub>H<sub>8</sub> isomers. Special thanks to Dr. Dorian Parker (University of Hawaii) for preparing Figure 4.

## REFERENCES

- (1) Kazakov, A.; Frenklach, M. On the Relative Contribution of Acetylene and Aromatics to Soot Particle Surface Growth. *Combust. Flame* **1998**, *112*, 270–274.
- (2) Frenklach, M. Reaction Mechanism of Soot Formation in Flames. *Phys. Chem. Chem. Phys.* **2002**, *4*, 2028–2037.
- (3) Frenklach, M.; Feigelson, E. D. Formation of Polycyclic Aromatic Hydrocarbons in Circumstellar Envelopes. *Astrophys. J.* **1989**, *341*, 372–384.
- (4) Unterreiner, B. V.; Sierka, M.; Ahlrichs, R. Reaction Pathways for Growth of Polycyclic Aromatic Hydrocarbons under Combustion Conditions, a DFT Study. *Phys. Chem. Chem. Phys.* **2004**, *6*, 4377–4384.
- (5) Fascella, S.; Cavallotti, C.; Rota, R.; Carra, S. Quantum Chemistry Investigation of Key Reactions Involved in the Formation of Naphthalene and Indene. *J. Phys. Chem. A* **2004**, *108*, 3829–3843.
- (6) Vereecken, L.; Bettinger, H. F.; Peeters, J. Reactions of Chemically Activated C<sub>9</sub>H<sub>9</sub> Species. Part I. The Product Distribution of the Reaction of Phenyl Radicals with Propyne. *Phys. Chem. Chem. Phys.* **2002**, *4*, 2019–2027.
- (7) Vereecken, L.; Peeters, J. Reactions of Chemically Activated C<sub>9</sub>H<sub>9</sub> Species II: The Reaction of Phenyl Radicals with Allene and Cyclopropene, and of Benzyl Radicals with Acetylene. *Phys. Chem. Chem. Phys.* **2003**, *5*, 2807–2817.
- (8) Vereecken, L.; Peeters, J.; Bettinger, H. F.; Kaiser, R. I.; Schleyer, P. v. R.; Schaefer, H. F., III. Reaction of Phenyl Radicals with Propyne. *J. Am. Chem. Soc.* **2002**, *124*, 2781–2789.
- (9) Gu, X.; Zhang, F.; Guo, Y.; Kaiser, R. I. Reaction Dynamics of Phenyl Radicals (C<sub>6</sub>H<sub>5</sub>, X<sup>2</sup>A<sub>1</sub>) with Methylacetylene (CH<sub>3</sub>CCH(X<sup>1</sup>A<sub>1</sub>)), Allene (H<sub>2</sub>CCCH<sub>2</sub>(X<sup>1</sup>A<sub>1</sub>)), and Their D4-Isotopomers. *J. Phys. Chem. A* **2007**, *111*, 11450–11459.
- (10) Kohn, D. W.; Clauberg, H.; Chen, P. Flash Pyrolysis Nozzle for Generation of Radicals in a Supersonic Jet Expansion. *Rev. Sci. Instrum.* **1992**, *63*, 4003–4005.
- (11) Kaiser, R. I.; Belau, L.; Leone, S. R.; Ahmed, M.; Wang, Y.; Braams, B. J.; Bowman, J. M. A Combined Experimental and Computational Study on the Ionization Energies of the Cyclic and Linear C<sub>3</sub>H Isomers. *Chem. Phys. Chem.* **2007**, *8*, 1236–1239.
- (12) Kaiser, R. I.; Mebel, A.; Kostko, O.; Ahmed, M. On the Ionization Energies of C<sub>4</sub>H<sub>3</sub> Isomers. *Chem. Phys. Lett.* **2010**, *485*, 281–285.
- (13) Selby, T. M.; Jasper, A. W.; Klippenstein, S. J.; Taatjes, C. A.; Goulay, F.; Soorkia, S.; Ray, A.; Osborn, D. L. An Experimental and Computational Study of the Product Branching Ratios in the Reaction of Phenyl Radical with Propargyl Radical. Manuscript in preparation.
- (14) Gusten, H.; Klasinc, L.; Ruscic, B. Photoelectron Spectroscopy of Heterocycles. Indene Analogs. *Z. Naturforsch. A* **1976**, *31*, 1051.
- (15) Kamphus, M.; Braun-Unkhoff, M.; Kohse-Hoeinghaus, K. Formation of Small PAHs in Laminar Premixed Low-Pressure Propene and Cyclopentene Flames: Experiment and Modeling. *Combust. Flame* **2008**, *152*, 28–59.
- (16) Li, Y.; Zhang, L.; Tian, Z.; Yuan, T.; Zhang, K.; Yang, B.; Qi, F. Investigation of the Rich Premixed Laminar Acetylene/Oxygen/Argon Flame: Comprehensive Flame Structure and Special Concerns of Polyynes. *Proc. Combust. Inst.* **2009**, *32*, 1293–1300.
- (17) Li, Y.; Zhang, L.; Yuan, T.; Zhang, K.; Yang, J.; Yang, B.; Qi, F.; Law, C. K. Investigation on Fuel-Rich Premixed Flames of Monocyclic Aromatic Hydrocarbons: Part I. Intermediate Identification and Mass Spectrometric Analysis. *Combust. Flame* **2010**, *157*, 143–154.
- (18) Li, Y.; Zhang, L.; Tian, Z.; Yuan, T.; Wang, J.; Yang, B.; Qi, F. Experimental Study of a Fuel-Rich Premixed Toluene Flame at Low Pressure. *Energy Fuels* **2009**, *23*, 1473–1485.
- (19) Li, Y.; Cai, J.; Zhang, L.; Yuan, T.; Zhang, K.; Qi, F. Investigation on Chemical Structures of Premixed Toluene Flames at Low Pressure. *Proc. Combust. Inst.* **2011**, *33*, 593–600.
- (20) Li, Y.; Cai, J.; Zhang, L.; Yang, J.; Zhang, K.; Qi, F. Experimental and Modeling Investigation on Premixed Ethylbenzene Flames at Low Pressure. *Proc. Combust. Inst.* **2011**, *33*, 617–624.
- (21) Nicolas, C.; Shu, J.; Peterka, D. S.; Hochlaf, M.; Poisson, L.; Leone, S. R.; Ahmed, M. Vacuum Ultraviolet Photoionization of C<sub>3</sub>. *J. Am. Chem. Soc.* **2006**, *128*, 220–226.
- (22) Hanley, L.; Zimmermann, R. Light and Molecular Ions: The Emergence of Vacuum UV Single-Photon Ionization in MS. *Anal. Chem.* **2009**, *81*, 4174–4182.
- (23) Baboul, A. G.; Curtiss, L. A.; Redfern, P. C.; Raghavachari, K. Gaussian-3 Theory Using Density Functional Geometries and Zero-Point Energies. *J. Chem. Phys.* **1999**, *110*, 7650–7657.
- (24) Curtiss, L. A.; Raghavachari, K.; Redfern, P. C.; Baboul, A. G.; Pople, J. A. Gaussian-3 Theory Using Coupled Cluster Energies. *Chem. Phys. Lett.* **1999**, *314*, 101–107.
- (25) Curtiss, L. A.; Raghavachari, K.; Redfern, P. C.; Rassolov, V.; Pople, J. A. Gaussian-3 (G3) Theory For Molecules Containing First and Second-Row Atoms. *J. Chem. Phys.* **1998**, *109*, 7764–7776.
- (26) Frisch, M. J.; Trucks, G. W.; Schlegel, H. B.; Scuseria, G. E.; Robb, M. A.; Cheeseman, J. R.; Zakrzewski, V. G.; Montgomery, J. A.; Stratmann, R. E.; Burant, J. C. et al. *Gaussian 98*, revision A.11; Gaussian, Inc.: Pittsburgh, PA, 2001.
- (27) MOLPRO, a package of *ab initio* programs designed by Werner, H.-J.; Knowles, P. J.; Amos, R. D.; Bernhardsson, A.; Berning, A.; Celani, P.; Cooper, D. L.; Deegan, M. J. O.; Dobbyn, A. J.; Eckert, F.; Hampel, C.; et al. version 2002.1.

## NOTE ADDED AFTER ASAP PUBLICATION

This paper was published ASAP on June 28, 2011. Ref 13 was added. The revised paper was reposted on July 11, 2011.